Particle and momentum balance during edge biasing in RFX

L. Tramontin[1], V. Antoni[1,2], M. Bagatin[1,2], L. Carraro[1], R. Cavazzana[1], D. Desideri[1,2], A. De Lorenzi[1], L. Garzotti[1], P. Innocente[1], R. Lorenzini[1], E. Martines[1], R. Pasqualotto[1], G. Serianni[1], M. Spolaore[1], N. Vianello[1]

[1]*Consorzio RFX, corso Stati Uniti 4, 35127 Padova, Italy*
[2]*INFM, Unità di Padova, Sez. A, Italy*

Negative edge biasing experiments performed in the reversed field pinch device RFX (R = 2 m, a = 0.457 m) have demonstrated that a modification of the toroidal rotation in the external region of the plasma induces a reduction of the electrostatic particle flux. The transport decrease is mainly led by the change in phase between density and plasma potential fluctuations [1]. During negative edge biasing the radial electric field becomes more negative and its shear increases by a factor of two. The electrostatic transport reduction is accompanied by an increase of the electron density as measured by two interferometers at different toroidal locations. In this paper two issues related to the effect of plasma edge polarisation will be discussed: the interpretation of the modification of the toroidal velocity by applying a momentum balance equation and the discharge particle balance taking into account the impurity contribution.

Two electrodes, made of a carbon-carbon composite head sustained by a molybdenum alloy shaft insulated from the plasma by a boron nitride case [2], have been inserted into the plasma up to r/a ≈ 0.8. They are designed to carry a 10-kA impulsive current each. The current is driven by a power supply based on capacitor banks. In this experimental campaign the current pulse of each electrode lasted for 20 ms. The electrodes were located in two different toroidal positions (φ = 142° and 322°). Figure 1 shows an example of plasma waveforms during negative edge biasing with the electrode at 322°. As in all RFX discharges the plasma column is toroidally distorted due to the non linear interaction of MHD modes locked in phase to the wall [3]. The picture illustrates the plasma current, the toroidal angle of the locked mode perturbation, the electrode current, the radiated power, the line-average electron density and the H_α emission in three toroidal positions (22°, 82° and 172°).

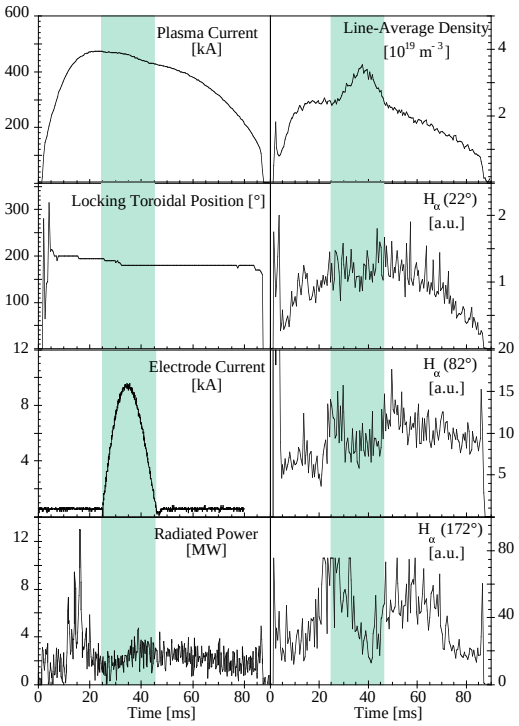

Fig. 1: Plasma waveforms during negative edge biasing (# 13634).

The radial behaviour of plasma toroidal flow, before and during edge biasing, is interpreted by applying a momentum balance equation for a single fluid [4], in analogy to what has been done in tokamaks [5]. The equation has been written in cylindrical coordinates (r,θ,z) and solved in stationary conditions by assuming azimuthal and axial symmetry. The ion viscosity accounts for the viscosity term and the dominant term in electron/ion collisions with neutrals is the ion-neutral charge exchange. The radial velocity u_r is taken as $-D(1/n)(dn/dr)$ where n is the density and D is the anomalous particle diffusion coefficient as derived from electrostatic fluxes and density gradient. The momentum balance equation for a single fluid in the axial direction is:

$$J_r B = nM\nu u_z - nMD\frac{1}{n}\frac{dn}{dr}\frac{du_z}{dr} + (\nabla\cdot\Pi_i)_z$$

where J_r is the radial current density, M is the ion

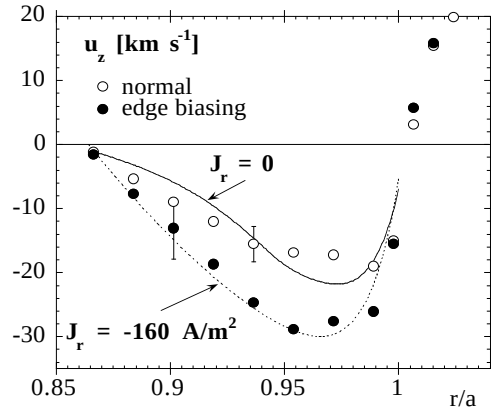

Fig. 2: Comparison of experimental data and simulations of the toroidal component of the plasma flow.

mass, u_z is the axial component of the flow velocity, Π_i is the ion viscosity tensor and ν is the ion/neutral charge-exchange frequency. With the assumptions reported in [4], the final form of the momentum balance equation in the axial direction is written in terms of density and temperature and their first order derivatives, and in terms of u_z and D and their first and second order derivatives. The toroidal component of the flow velocity, u_z, is obtained by numerically solving the resulting second order differential equation. The boundary conditions are the experimental values of u_z at r/a = 1 and r/a = 0.87. To take into account ion losses at the wall due to finite Larmor radius effects, a force term has been added in the balance equation, with a radial profile $F = F_0 \exp[-((r/a-1)/\sigma)^2]$, where F_0 is the value at the wall and σ represents its radial extension in normalised units [6]. The resulting u_z is compared with the value derived from the experimental data used in the Ohm's law in the radial direction. We have found a good agreement between experimental values of the toroidal plasma flow and the model, as shown in figure 2. The figure illustrates the toroidal component of the plasma velocity before ($J_r = 0$, $F_0/B = -300$ Am^{-2}, $\sigma = 0.04$) and during negative edge biasing ($J_r = -160$ Am^{-2}, $F_0/B = -100$ Am^{-2}, $\sigma = 0.04$). The value of F_0 has been changed consistently with the electrostatic particle flux that decreases during edge polarisation.

As shown in fig. 1, the density increases by 40% while the H_α signals remain constant or slightly decrease during negative edge biasing (discharge 13634). In this discharge the locked mode perturbation occurred at an angle of ~170° and its effect is visible in the H_α signal at 172° which saturates. Figure 3 shows the typical density profiles in normal condition and during negative edge biasing measured by a 13-chord mid-infrared vibration compensated system. The profiles become hollower, the density increases in the bulk and at the edge showing a peak at r/a ~0.8. The higher density is reached at 37.5 ms. The gradient at the edge steepens and this agrees with data from Langmuir probe measurements at the plasma edge. The typical electron temperature profile in a standard discharge, measured by Thomson Scattering, is well described by $T_e(r) = (T_0-T_a)(1-(r/a)^4) + T_a$ with on-axis temperature,T_0, of 150 eV and edge temperature, T_a, of 10 eV. During edge biasing the core temperature decreases to ~100 eV. Langmuir probes confirm a decrease of the edge temperature and a flattening of its gradient. Among all the discharges with edge polarisation, some of them show some features of a possible improvement of the particle confinement, i.e. density rise, steepening of the density gradient and a slight decrease of H_α emission. For these discharges the electrons due to impurity contamination have been estimated. The main contribution is given by boron and nitrogen. In fact, while the emissions of C and O roughly follow the density time behaviour, the emissions of B and N increase more rapidly than density. In order to evaluate the electron density from B and N, the time evolutions and the intensities of selected measured lines have been compared with the results of a 1-dimensional collisional-radiative code [7]. The selected lines are the BIV line at 2822 Å and the resonant line

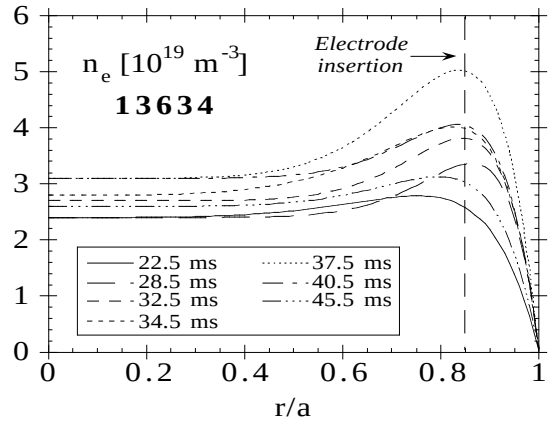

Fig. 3: Density profiles during edge biasing.

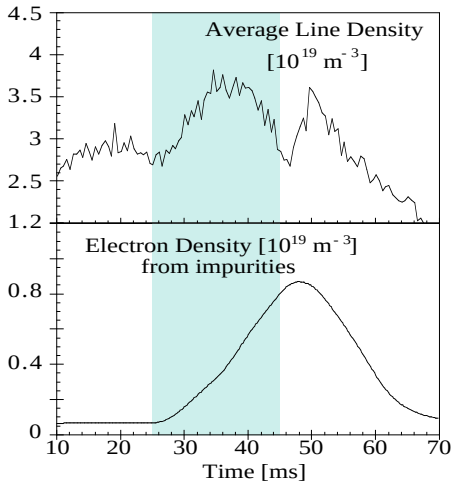

Fig. 4: Line-average electron density and electron density due to impurity during the electrode action

of NVI at 29 Å, measured with absolutely calibrated spectrographs [8] and time resolutions of 2 and 20 ms respectively; the NIV line at 3479 Å, measured with a non absolutely calibrated spectrograph with time resolution of 2 ms. The electron density due to impurity, plotted as a function of time in figure 4 for discharge 13637, reaches a maximum value at ~47 ms corresponding to the switch off of the power applied to the electrode. It is worth noting that the impurity content is at maximum ~10 ms after the maximum value of electron density.

A 0-dimensional model, already applied to RFX data [9], simulates the temporal behaviour of the plasma particle inventory. Two reservoirs, the plasma and the wall, are considered and the temporal behaviour of hydrogen is described by two coupled differential equations, $\frac{\partial N_p}{\partial t} = -(1-R)\frac{N_p}{\tau_p} + \frac{N_w}{\tau_w}$ and $\frac{\partial N_w}{\partial t} = (1-R)\frac{N_p}{\tau_p} - \frac{N_w}{\tau_w}$ where N_p is the total plasma particle content, N_w is the wall inventory, τ_p is the particle confinement time in the plasma, τ_w is a characteristic time the wall and R = 0.5 is the reflection coefficient for H in graphite. N_p results from the integration of the electron density profiles, once the electrons due to impurities have been subtracted; N_w derives from considerations on the quantity of hydrogen adsorbed into the graphite and is limited by the saturation level of hydrogen in graphite. The particle confinement time, τ_p = 1.2 ms, is obtained from a particle balance in the stationary phase, when the particle influx from H_α emission and the particle flux from electrostatic fluctuations are comparable and of the order of $5 \cdot 10^{21}$ m^{-2}s^{-1}. The characteristic time of the wall, τ_w, is adjusted to simulate the pre-biasing equilibrium phase and depends on N_w. Figure 5 shows the result of the simulation of the hydrogen density in the discharge 13637. The values of N_w and τ_w, before edge biasing, are respectively $40 \cdot 10^{20}$ particles and 42 ms. The simulation follows the density time evolution if the particle confinement time is allowed to change, while τ_w is nearly constant. The best agreement is reached when τ_p changes linearly from 1.2 ms to a value ~35% higher, during the electrode current rise between 26 and 35 ms. To reproduce the density decrease, τ_p is changed linearly from the higher value down to 0.9 ms at 44 ms. The lower value of τ_p at the end of the electrode operation indicates that a competition exists between the reduction of transport and the contamination of the plasma due to impurities.

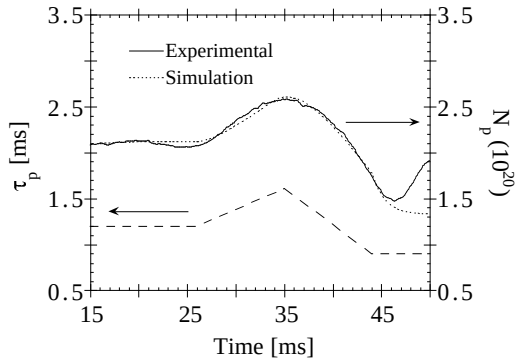

Fig. 5: Simulation of the particle density with a 0-D model.

The radial density profiles have also been interpreted by means of a 1-dimensional particle transport model [10]. The model is made up of two parts: one for the solution of the continuity equation giving the evolution of the ion density profiles, and the other one for the calculation of the neutral density inside the discharge. The particle flux is written as $\Gamma(r,t) = -D(r)\,\partial n(r,t)/\partial r + V(r)n(r,t)$ where D(r) and V(r) are the diffusion coefficient and the pinch

velocity respectively. The aim of the analysis is to determine the values of D(r) and V(r) giving the best simulations of the electron density profile. The diffusion coefficient consists of two components, one related to the transport mechanisms inside the core governed by magnetic fluctuations (stochastic transport) and the other related to the electrostatic particle flux which is the main mechanism of particle transport at the edge. The global convective flux includes, in addition to the inward $E_\phi B_\theta$ drift, an outward directed term proportional to the temperature gradient. Both the stochastic and electrostatic diffusion profiles are given as an input to the code and adjusted to obtain a particle flux comparable to the experimental value (electrostatic flux). The temperature profiles have been assumed in agreement with the experimental data with $T_e(r) = T_i(r) = T(r)$. The code has been applied to simulate stationary conditions (Fig. 6). As already reported [10], an outward directed fluid velocity is necessary to reproduce the hollow density profiles observed in the pre-biasing phase. The diffusion coefficient in the core is 28 m^2s^{-1} and decreases to 4.5 m^2s^{-1} at the edge. To simulate the density radial behaviour during edge polarisation we changed the temperature profile, and thus the pinch velocity, according to the experimental values. We also required that the value of D in the core did not change assuming that edge biasing does not affect the magnetic transport. The diffusion coefficient at the edge is thus reduced by a factor of ~3 in agreement with the reduction of the electrostatic particle flux. In the frame of this model the experimental results are consistent with a reduction of the transport at the edge, while it has not been necessary to modify the core transport in order to reproduce the density profiles. On the other hand, the 0-D model gives an increase of 35% of τ_p. Comparing these results it emerges that a transport mechanism other than electrostatic fluctuations has to be introduced in the particle balance and this term is identified with the parallel losses and the density refueling due to the locked modes.

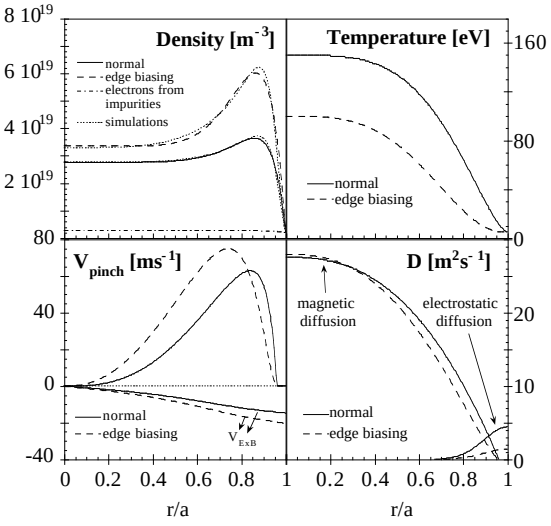

Fig. 6 1-D simulations of density profiles.

Acknowledgements
The authors wish to thank Dr. M. Mattioli for providing nitrogen simulations.

[1] V. Antoni *et al.*, Plasma Physics and Controlled Fusion **42**, 83 (2000)
[2] D. Desideri, A. De Lorenzi and P. Zaccaria, Fusion Eng. and Design, **45**, 455 (1999)
[3] P. Zanca and S. Martini, Plasma Physics and Controlled Fusion **41**, 1251 (1999)
[4] D. Desideri *et al.*, Czech. J. Phys. **49 S3**, 119 (1999)
[5] J. Cornelis, R. Sporken, G. Van Oost and R. R. Weynants, Nucl. Fusion **34**, 171 (1994)
[6] F. Sattin *et al*. to be presented to the 3rd Europhysics Workshop on the Role of Electric Fields in Plasma Confinement and Exhaust, Budapest, June18-19, 2000
[7] L. Carraro *et al*., Nucl. Fusion **36**, 1623 (1996)
[8] L. Carraro *et al*., Rev. Sci. Instrum. **66**, 613 (1995)
[9] L. Garzotti *et al.*, 1998 ICPP & 25th EPS Conf. on Contr. Fusion and Plasma Physics, Praha Vol. 22C, 782 (1998)
[10] D. Gregoratto, L. Garzotti, P. Innocente, S. Martini and A. Canton, Nucl. Fusion **38**, 1199 (1998)